ChemComm

COMMUNICATION

View Article Online
View Journal | View Issue

Check for updates

Cite this: *Chem. Commun.*, 2019, 55, 11430

Received 26th July 2019,
Accepted 28th August 2019

DOI: 10.1039/c9cc05836b

rsc.li/chemcomm

Published on 29 August 2019. Downloaded by Utah State University on 10/11/2019 3:42:01 PM.

# Redox switchable catalysis utilizing a fluorescent dye†

Brena L. Thompson,[a] Casey R. Simons[b] and Zachariah M. Heiden *[a]

**This report describes the implementation of a 4,4-difluoro-4-bora-3*a*,4*a*-diaza-*s*-indacene (BODIPY) dye into the ligand framework of a Rh-based catalyst. The redox-active nature of the BODIPY dye is utilized to generate a catalyst that is capable of exhibiting redox-switchable catalytic behavior for the hydroboration of alkenes through a BODIPY-based reduction.**

With the advent of more complex chemical products, the development of switchable catalysts capable of turning a chemical reaction "on" or "off" with controlled timing is critical to maximizing the yield of the desired product and minimizing undesired chemical reactions.[1] One of the mechanisms for switchable reactivity involves the control of oxidation state with redox-active ligands.[1] Although many ligand frameworks have been utilized in switchable reactivity with redox-active ligands,[1,2] fluorescent dye molecules represent an exciting new opportunity, as they exhibit reversible electrochemistry in the absence of a metal,[3] can be readily synthesized,[4] are biologically compatible,[5] and can even promote electron transfer when illuminated.[6] One dye molecule that has received recent attention for its ability to exhibit reversible electrochemistry and tunable redox potentials is the metal-free 4,4-difluoro-4-bora-3*a*,4*a*-diaza-*s*-indacene (BODIPY) dye.[7,8]

A few groups have implemented BODIPY molecules in metal complexes for uses beyond medicinal applications.[9–11] Higham and coworkers have shown that BODIPY-containing phosphines can be used to generate Ag, Au, and Cu complexes, but the electron deficient nature of the BODIPY fragment generates phosphine compounds that are weak ligands.[12] Plenio and coworkers have generated BODIPY containing phosphines and N-heterocyclic carbenes for the investigation of catalyst intermediates.[13–16] BODIPY dyes have also been recently incorporated into a Pt complex for singlet $O_2$ detection.[17–19] Although BODIPY dyes have been incorporated into metal complexes, the redox character of the BODIPY dye has not been utilized to control metal center reactivity.

Rhodium-based complexes have been shown to be capable catalysts for hydrogenations,[20] hydrosilylations,[21] hydroborations,[22] hydroacylations,[23] and many other reactions. The breadth of reactivity of rhodium complexes makes rhodium an attractive choice as a metal center for the investigation of switchable reactivity. Wrighton and coworkers have reported that the catalytic activity of a rhodium complex containing a cobaltocene center in the ligand framework can switch the catalyst selectivity between the hydrogenation and hydrosilylation of alkenes.[24] As expected, oxidation of the cobaltocene center generates a more Lewis acidic rhodium center, making oxidative addition of $H_2$ at the rhodium center less favorable.

To generate a bidentate phosphine containing a BODIPY dye, bis[2-(diphenylphosphino)ethyl]ammonium chloride was treated with 8-methylthio-BODIPY (BoSMe) in the presence of one

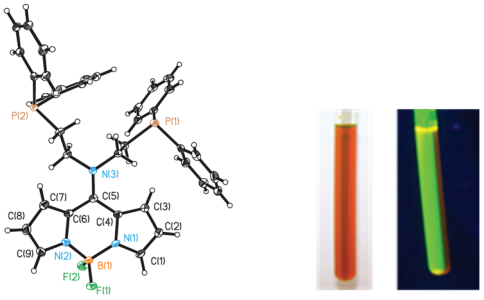


Fig. 1 (left) Molecular structure of BoPNP. Thermal ellipsoids are drawn at 50% probability. Key bond distance and angle: N(3)–C(5) = 1.341(2) Å, dihedral of C(2)–C(5)–B(1)–C(8) = 162.94(14)°. Pictures of NMR tubes showing BoPNP in $CD_2Cl_2$ under (middle) ambient light and (right) UV light.

[a] *Department of Chemistry, Washington State University, Pullman, WA 99164, USA. E-mail: zachariah.heiden@wsu.edu*

[b] *Department of Chemistry and Biochemistry, Utah State University, Logan, UT 84322, USA*

† Electronic supplementary information (ESI) available: Synthetic methods, catalytic conditions and results, photographs of the catalytic reactions, multinuclear NMR spectra of BoPNP and [(COD)Rh(BoPNP)]$BF_4$, details of molecular structure analysis, cyclic voltammograms, normalized absorbance and emission spectra, sample input file for Gaussian09, free energies for the hydroboration of alkenes, gas phase energies, molecular orbitals, and 3D coordinates of all computed structures. CCDC 1861895 and 1939653. For ESI and crystallographic data in CIF or other electronic format see DOI: 10.1039/c9cc05836b



This journal is © The Royal Society of Chemistry 2019

Published on 29 August 2019. Downloaded by Utah State University on 10/11/2019 3:42:01 PM.

equivalent of triethylamine generating 8-(bis[2-(diphenylphosphino)ethyl]amine)-BODIPY (BoPNP) in a 68% yield (eqn (1)). When illuminated with UV light, the resulting red colored solid fluoresced yellow in the solid-state and green when dissolved in methylene chloride (Fig. 1). The presence of a singlet at −20.8 ppm in the $^{31}P\{^{1}H\}$ NMR spectrum, a 1 : 1 : 1 : 1 quartet at −149.1 ppm with a $^{1}J_{BF}$ coupling of 23 Hz in the $^{19}F$ NMR spectrum, and a triplet at 0.09 ppm with a $^{1}J_{BF}$ = 23 Hz coupling constant in the $^{11}B$ NMR spectrum verified the addition of a BODIPY fragment to the amine center of bis[2-(diphenylphosphino)ethyl]amine.

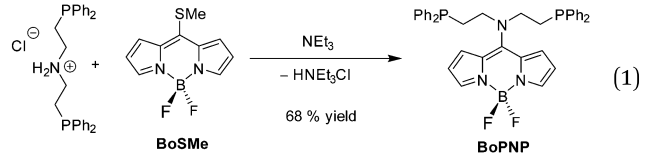


(1)

To examine the nature of a BODIPY dye incorporated into the BoPNP ligand, X-ray quality crystals of BoPNP were grown by vapor diffusion of pentanes into a methylene chloride solution of BoPNP. X-ray crystallographic analysis revealed a BODIPY dye that deviated about 17° from planarity (C(2)–C(5)–B(1)–C(8) dihedral angle). The deviation of the pyrrole rings is an important property as the planarity of the BODIPY core and the extended π-system are predominantly responsible for the optical properties of 8-amino-BODIPYs.[25] BoPNP was found to be soluble in most organic solvents, air stable in the solid state, and moderately air stable in solution.

To generate a Rh complex from BoPNP, 1.2 equivalents of BoPNP was treated with one equivalent of $[(COD)_2Rh]BF_4$, where COD = *cis*-1,5-cyclooctadiene, generating $[(COD)Rh(BoPNP)]BF_4$ in 63% yield (eqn (2)). The orange colored $[(COD)Rh(BoPNP)]BF_4$ fluoresced yellow green under UV light in THF (Fig. 2). The generation of the desired rhodium complex was demonstrated by the presence of a triplet at 0.17 ppm in the $^{11}B\{^{1}H\}$ NMR spectrum, a quartet at −147.2 ppm in the $^{19}F$ NMR spectrum, and a broad doublet at 26.5 ppm ($^{1}J_{RhP}$ = 146 Hz) in the $^{31}P\{^{1}H\}$ NMR spectrum, which is characteristic of coordination of the BoPNP to a Rh center.

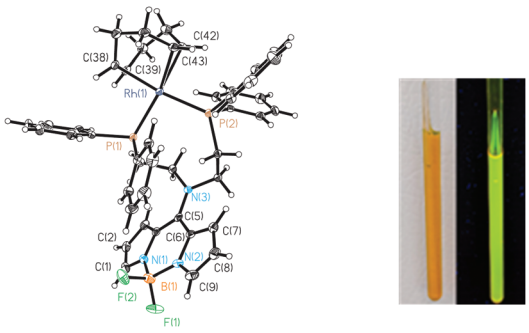


Fig. 2 (left) Molecular structure for $[(COD)Rh(BoPNP)]^+$. Thermal ellipsoids are drawn at 50% probability. The $BF_4^-$ anion and $CH_2Cl_2$ solvent molecules are omitted for clarity. (middle) NMR tubes containing $[(COD)Rh(BoPNP)]BF_4$ in THF (right) under ambient light, and (right) under UV light. Key bond distances and angles: Rh–P(1) = 2.3124(8) Å, Rh–P(2) = 2.3500(8) Å. P(1)–Rh–P(2) = 96.48(3)°. Dihedral of C(2)–C(5)–B(1)–C(8) = 172.1(5)°.

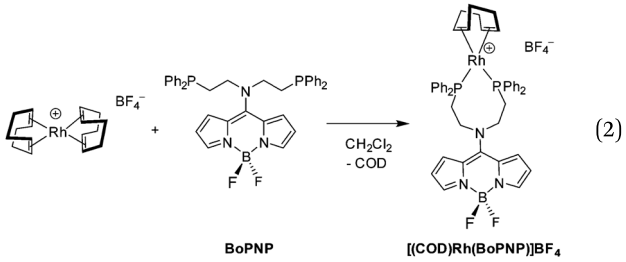


(2)

Investigation of the photophysical properties of $[(COD)Rh(BoPNP)]BF_4$ yielded two absorptions of 344 and 431 nm and an emission at 538 nm in $CH_2Cl_2$ (see ESI†), which are only slightly shifted (2–3 nm bathochromic shift) from the free ligand ($\lambda_{abs}$ = 340 and 428 nm, $\lambda_{emission}$ = 536 nm). Although the quantum yield of $[(COD)Rh(BoPNP)]BF_4$ was low at 0.072, it was about two times greater than free BoPNP ($\Phi$ = 0.042) in $CH_2Cl_2$. The excited state lifetimes ($\tau$ = 4.4 and 5.5 ns in $CH_2Cl_2$) of $[(COD)Rh(BoPNP)]BF_4$ were almost identical to free BoPNP ($\tau$ = 2.6 and 5.7 ns). Due to the similarity between the photophysical properties of $[(COD)Rh(BoPNP)]BF_4$ and free BoPNP, the photophysical properties of $[(COD)Rh(BoPNP)]BF_4$ are attributed to the BODIPY dye, as opposed to the Rh center.

The generation of $[(COD)Rh(BoPNP)]BF_4$ was further verified by crystallographic analysis. X-ray quality crystals were grown by the diffusion of pentanes into a dichloromethane solution at −30 °C. Crystallographic analysis revealed the presence of a square planar rhodium center containing a bidentate BoPNP ligand with a bite angle of 96.48(3)° and an $\eta^4$-COD ligand with the average Rh–C distance of 2.234 Å. The BODIPY fragment of $[(COD)Rh(BoPNP)]BF_4$ deviates about 8° from planarity, which is about 10° less than the free ligand.

Electrochemical analysis of a THF solution of $[(COD)Rh(BoPNP)]BF_4$ showed a quasireversible reduction at −1.65 V *vs.* $Cp_2Fe/Cp_2Fe^+$ (+122 mV from BoPNP). The reduction potential of BoPNP (−1.77 V) is about 200 mV more negative than the average reduction potential (−1.53 V) for a BODIPY dye.[7] The single reversible wave near the reduction of the free ligand likely suggests that the reduction wave occurs at the BODIPY center of the Rh complex. Reduction of the BODIPY dye instead of the Rh center suggests that the BODIPY-based redox event could be utilized to alter the reactivity at the Rh center.

To further verify that a redox event would result in a BODIPY-based reduction, $[(COD)Rh(BoPNP)]BF_4$ was treated with 1.1 equiv. $KC_8$ in THF (eqn (3)), resulting in a red orange ($\lambda_{abs}$ = 338 and 422 nm) colored solution that did not fluoresce under UV light. EPR analysis of the reaction product in THF at 90 K revealed a *g*-value of 2.005 (Fig. 3). Due to the absence of hyperfine splitting, at RT or 90 K, the EPR results suggest the presence of a carbon-based (BODIPY-based) radical. We have also observed a carbon-based radical in the reduction of a tetramethylguanidine-appended BODIPY dye.[8] If a rhodium-based radical as opposed to an organic-based radical had formed from the reduction of $[(COD)Rh(BoPNP)]BF_4$ a doublet and a *g*-value shifted away from 2.005 would have been observed.[26,27] Based on these results the reduction product of $[(COD)Rh(BoPNP)]BF_4$ is assigned as the

Published on 29 August 2019. Downloaded by Utah State University on 10/11/2019 3:42:01 PM.

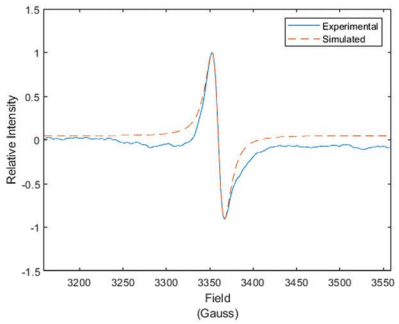


Fig. 3 EPR spectrum of a THF solution of [(COD)Rh(BoPNP)] at 90 K.

zwitterionic complex, [(COD)Rh(BoPNP)] (eqn (3)). Crystallization attempts of [(COD)Rh(BoPNP)] resulted in crystals that did not diffract.

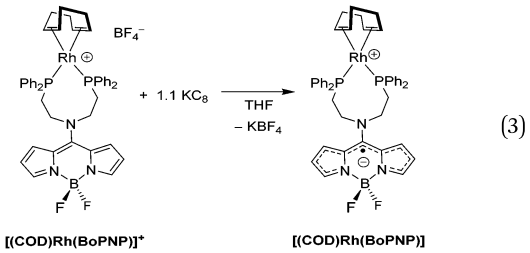


(3)

To investigate the catalytic activity of [(COD)Rh(BoPNP)]$BF_4$, the catalytic hydrogenation (4 atm of $H_2$) of limonene, the hydrosilylation of limonene with $Ph_2SiH_2$, the hydroboration of styrene with pinacolborane, and the hydroacylation of 2,2-dimethyl-4-pentenal were undertaken with 1.5 mol% catalyst for 24 hours at 23 °C. Only the hydroboration reaction resulted in complete conversion. Attempting the same catalytic reactions with [(COD)Rh(BoPNP)], as opposed to [(COD)Rh(BoPNP)]$BF_4$, showed no conversion in any of the catalytic reactions, suggesting that the addition of an electron to the BODIPY dye can be utilized to turn "off" the catalytic activity of [(COD)Rh(BoPNP)]$BF_4$.

The catalytic activity of [(COD)Rh(BoPNP)]$BF_4$, for the hydroboration of styrene, was further examined (Table 1). THF and $CH_2Cl_2$ were superior solvents to acetone and acetonitrile (see ESI†). Although similar catalytic results for the hydroboration of styrene were obtained with catecholborane or pinacolborane, pinacolborane was chosen for further investigations. Hydrolysis of the hydroboration products resulted in a 7 : 1 ratio of 1-phenylethanol : 2-phenylethanol.

To probe the substrate scope for the catalytic hydroboration of alkenes with [(COD)Rh(BoPNP)]$BF_4$, the hydroboration of five alkenes was examined (Table 2). The hydroboration of 1-hexene occurred twice as fast as styrene. No conversion for the hydroboration of (+)-limonene, α-pinene, or β-pinene with pinacolborane was observed. Under the same reaction conditions, the hydroboration of (+)-limonene with 0.83 equivalents of catecholborane resulted in the hydroboration of only the terminal alkene. Addition of a second equivalent of catecholborane did not result in the hydroboration of the internal alkene of (+)-limonene. The catalytic hydroboration of α-pinene or β-pinene with catecholborane led to the complete hydroboration of β-pinene and no conversion of α-pinene over 24 hours. Hydrolysis of the hydroboration products of β-pinene resulted in a 1 : 1 ratio of the myrtanol diastereomers. The increased reactivity for the hydroboration of sterically bulky alkenes with catecholborane, as opposed to pinacolborane, is attributed to the decreased steric bulk of catecholborane when compared to pinacolborane.

Table 1 Catalytic hydroboration of (0.115 mmol) styrene with [(COD)Rh(BoPNP)]$BF_4$ with 0.83 equivalents of pinacolborane in THF at 23 °C. Conversion was determined by NMR spectroscopy

| Catalyst concentration (mol%) | Time (hours) | Conversion (%) |
|---|---|---|
| 0.1 | 24 | 0 |
| 0.5 | 24 | 20 |
| 1.0 | 10 | 100 |
| 3.0 | 4 | 100 |
| 5.0 | 0.5 | 100 |

Table 2 Substrate scope for the hydroboration of (0.088–0.115 mmol) alkenes with 3 mol% [(COD)Rh(BoPNP)]$BF_4$ with 0.83 equivalents of pinacolborane (HBpin) or catecholborane (HBcat) in THF at 25 °C. Conversion was determined by NMR spectroscopy

| Alkene | Time (hours) | Borane | Conversion (%) |
|---|---|---|---|
| Styrene | 4 | HBpin | 100 |
| 1-Hexene | 2 | HBpin | 100 |
| (+)-Limonene | 24 | HBpin | 0 |
| (+)-Limonene | 24 | HBcat | 100 |
| α-Pinene | 24 | HBpin | 0 |
| α-Pinene | 24 | HBcat | 0 |
| β-Pinene | 24 | HBpin | 0 |
| β-Pinene | 24 | HBcat | 100 |

Since [(COD)Rh(BoPNP)]$BF_4$ was catalytically active for the hydroboration of styrene with pinacolborane and [(COD)Rh(BoPNP)] was not, the sequential addition of a reductant and an oxidant was hypothesized to be able to toggle between an active and inactive catalyst (eqn (4)). The catalytic hydroboration of styrene was allowed to proceed for 1 hour, resulting in a 35% conversion. Then, 0.95 equiv. of $Cp^*_2Co$ was added, resulting in [(COD)Rh(BoPNP)], and an additional 2% conversion in the hydroboration of styrene occurred over the next hour (Fig. 4). 0.95 equiv. $[Cp_2Co]PF_6$ was then added, regenerating $[(COD)Rh(BoPNP)]^+$, and an additional 40% of conversion for the hydroboration of styrene resulted. Repeating this procedure for an additional cycle lead to the complete hydroboration of styrene over 3.5 hours. The use of an oxidant stronger than $[Cp_2Co]^+$ resulted in the oxidation of pinacolborane as opposed to [(COD)Rh(BoPNP)]. This fact suggests that catalysts that are capable of redox-switchable hydroborations require reduction potentials similar to $[Cp_2Co]^+$ to favor oxidation of the catalyst as opposed to the borane.

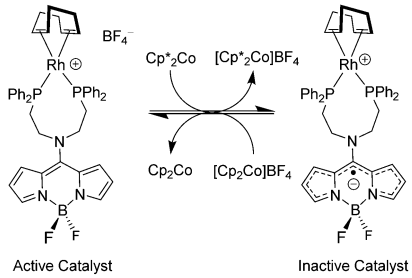


(4)


This journal is © The Royal Society of Chemistry 2019

Published on 29 August 2019. Downloaded by Utah State University on 10/11/2019 3:42:01 PM.

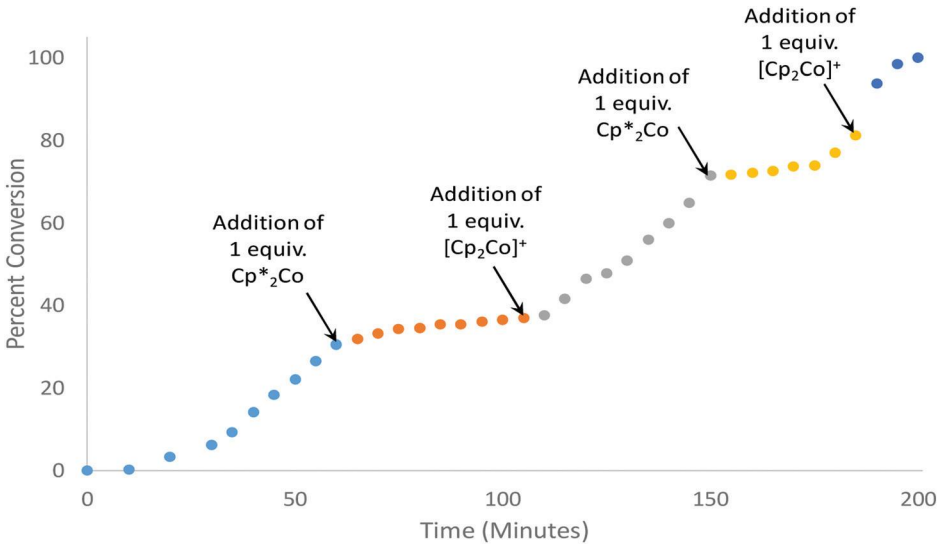


Fig. 4 Plot showing the conversion of the hydroboration of styrene with 3 mol% [(COD)Rh(BoPNP)]$BF_4$ when exposed to sequential additions of $Cp^*_2Co$ (reductant) and $[Cp_2Co]PF_6$ (oxidant).

These results show that the reduction of a BODIPY fragment can "turn off" the catalytic activity of an appended metal center, with the catalytic activity returning upon exposure to an oxidant. Although BODIPY fragments are capable of promoting chemical reactions when photolyzed, the BODIPY dye was not close enough to the Rh center to influence the catalytic activity when illuminated. The reported redox switchable behavior presents a new approach towards controlling catalytic reactions. The incorporation of BODIPY dyes into molecular scaffolds to influence catalytic reactivity is a topic of interest of our research group.

This research was supported by Washington State University and the Washington State University Seed Grant Program. We would also like to acknowledge the EPR facility at Utah State University. EPR spectra were collected using a Bruker EMXplus EPR spectrometer, principally supported by NSF MRI-0722849. We acknowledge the single crystal X-ray diffraction facility at the University of Montana (UM). X-ray diffraction studies were supported by the CBSD at UM (National Institutes of Health, CoBRE NIGMS P20GM103546) and the X-ray diffractometer was purchased in part through support from National Science Foundation (NSF)-MRI (CHE – 1337908).

## Conflicts of interest

There are no conflicts to declare.

## Notes and references

1 V. Blanco, D. A. Leigh and V. Marcos, *Chem. Soc. Rev.*, 2015, **44**, 5341–5370.
2 J. Wei and P. L. Diaconescu, *Acc. Chem. Res.*, 2019, **52**, 415–424.
3 A. B. Nepomnyashchii and A. J. Bard, *Acc. Chem. Res.*, 2012, **45**, 1844–1853.
4 A. Loudet and K. Burgess, *Chem. Rev.*, 2007, **107**, 4891–4932.
5 A. Kamkaew, S. H. Lim, H. B. Lee, L. V. Kiew, L. Y. Chung and K. Burgess, *Chem. Soc. Rev.*, 2013, **42**, 77–88.
6 G. Magagnano, A. Gualandi, M. Marchini, L. Mengozzi, P. Ceroni and P. G. Cozzi, *Chem. Commun.*, 2017, **53**, 1591–1594.
7 B. L. Thompson and Z. M. Heiden, in *Redox Chemistry of BODIPY Dyes. In BODIPY Dyes – A Privilege Molecular Scaffold with Tunable Properties*, ed. J. Bañuelos-Prieto and R. S. Llano, IntechOpen, 2018, pp. 45–64.
8 I. A. Kieffer, R. J. Allen, J. L. Fernandez, J. L. Deobald, B. L. Thompson, J. D. Wimpenny and Z. M. Heiden, *Angew. Chem., Int. Ed.*, 2018, **57**, 3377–3380.
9 A. M. Lifschitz, C. M. Shade, A. M. Spokoyny, J. Mendez-Arroyo, C. L. Stern, A. A. Sarjeant and C. A. Mirkin, *Inorg. Chem.*, 2013, **52**, 5484–5492.
10 A. M. Lifschitz, R. M. Young, J. Mendez-Arroyo, V. V. Roznyatovskiy, C. M. McGuirk, M. R. Wasielewski and C. A. Mirkin, *Chem. Commun.*, 2014, **50**, 6850–6852.
11 B. Bertrand, K. Passador, C. Goze, F. Denat, E. Bodio and M. Salmain, *Coord. Chem. Rev.*, 2018, **358**, 108–124.
12 L. H. Davies, R. W. Harrington, W. Clegg and L. J. Higham, *Dalton Trans.*, 2014, **43**, 13485–13499.
13 R. Vasiuta and H. Plenio, *Chem. – Eur. J.*, 2016, **22**, 6353–6360.
14 V. Sashuk, D. Schoeps and H. Plenio, *Chem. Commun.*, 2009, 770–772.
15 P. Kos and H. Plenio, *Angew. Chem., Int. Ed.*, 2015, **54**, 13293–13296.
16 P. Kos and H. Plenio, *Chem. – Eur. J.*, 2015, **21**, 1088–1095.
17 F. Geist, A. Jackel and R. F. Winter, *Inorg. Chem.*, 2015, **54**, 10946–10957.
18 P. Irmler and R. F. Winter, *Dalton Trans.*, 2016, **45**, 10420–10434.
19 P. Irmler and R. F. Winter, *Organometallics*, 2018, **37**, 235–253.
20 X. Cui and K. Burgess, *Chem. Rev.*, 2005, **105**, 3272–3296.
21 H. Brunner, *Angew. Chem.*, 1983, **95**, 921–931.
22 S. Pereira and M. Srebnik, *Tetrahedron Lett.*, 1996, **37**, 3283–3286.
23 M. C. Willis, *Chem. Rev.*, 2010, **110**, 725–748.
24 I. M. Lorkovic, R. R. Duff and M. S. Wrighton, *J. Am. Chem. Soc.*, 1995, **117**, 3617–3618.
25 C. A. Osorio-Martinez, A. Urias-Benavides, C. F. A. Gomez-Duran, J. Banuelos, I. Esnal, I. Lopez Arbeloa and E. Pena-Cabrera, *J. Org. Chem.*, 2012, **77**, 5434–5438.
26 B. de Bruin, J. C. Russcher and H. Gruetzmacher, *J. Organomet. Chem.*, 2007, **692**, 3167–3173.
27 J. Orsini and W. E. Geiger, *J. Electroanal. Chem.*, 1995, **380**, 83–90.